Tadeusz Stadnik, MD • Achille Stevenaert, MD • Albert Beckers, MD • Robert Luypaert, PhD •
Thérèse Buisseret, MD • Michel Osteaux, MD

Pituitary Microadenomas: Diagnosis with Two- and Three-dimensional MR Imaging at 1.5 T before and after Injection of Gadolinium[1]

The usefulness of different magnetic resonance (MR) imaging sequences (coronal and sagittal spin-echo [SE] and three-dimensional fast low-angle shot [3D FLASH]) in the detection of pituitary microadenomas before and after gadolinium injection was prospectively evaluated in 28 patients with surgical confirmation. When evaluated separately, the most useful sequences in the detection of these microadenomas were coronal pregadolinium T1-weighted SE, coronal pregadolinium 3D FLASH, coronal postgadolinium T1-weighted SE, and coronal postgadolinium 3D FLASH. The combination of pre- and postgadolinium T1-weighted sequences with pre- and postgadolinium 3D FLASH sequences produced the highest number of true-positive findings (90%) and the lowest number of false-positive findings (5%). When a 1.5-T imaging unit with a high signal-to-noise ratio allowing useful three-dimensional acquisition is used, the authors advocate a coronal T1-weighted SE sequence, followed (if necessary) by a coronal 3D FLASH sequence, both without injection of gadolinium, in the diagnosis of pituitary microadenomas. When no confident diagnosis is reached, the same sequences should be performed after the injection of gadolinium. The sagittal pre- and postgadolinium T1-weighted SE and long-TR SE sequences are useful only in specific cases.

HIGH-RESOLUTION high-magnetic-field magnetic resonance (MR) imaging is becoming widely accepted as the most sensitive imaging method in the diagnosis of pituitary microadenomas. A true-positive rate of 81%–100% has been reported in MR imaging at 1.5 T in the detection of microadenomas without injection of contrast material (1–4). Previous studies also suggest a higher rate of detection after gadolinium injection (5–8). The aim of this study was to evaluate different sequences and gadolinium injection in the diagnosis of pituitary microadenomas by means of optimized high-resolution, high-magnetic-field-strength MR imaging with the capability of three-dimensional acquisition. The use of three-dimensional acquisition is promising in the diagnosis of pituitary microadenomas. Indeed, the very small section thickness (up to 1 mm) and high signal-to-noise ratio of three-dimensional acquisition are important advantages with respect to the conventional spin-echo (SE) sequences (minimal section thickness of 2 mm produces a poor signal-to-noise ratio, to improve which necessitates four or eight excitations).

PATIENTS AND METHODS

Seventy-seven patients suspected of having microadenomas on the basis of clinical and/or computed tomographic (CT) findings were evaluated between September 1987 and April 1989 on a 1.5-T MR imaging unit (Magnetom; Siemens,

Erlangen, Federal Republic of Germany) that allowed three-dimensional acquisitions. Twenty-eight patients underwent a transsphenoidal exploration; this report covers only the data from these patients. The microadenoma was found during surgery in 27 patients (20 patients with a prolactinoma, six with an adrenocorticotropic hormone (ACTH)-secreting adenoma, and one patient with a growth-hormone–secreting microadenoma). In one patient with Cushing syndrome, only a multinodular hyperplasia was found. The indications for surgery in the patients with prolactinomas were the patient's preference for surgical removal of the microadenoma and the unsuccessful or ill-tolerated treatment with bromocriptine. The transsphenoidal resection was performed only if a focal abnormality and/or indirect signs of a microadenoma were present at CT and/or MR imaging conjointly with an abnormal prolactin level. In seven cases of Cushing syndrome clinically suspected to be of pituitary origin, the transsphenoidal exploration was started on the side of focal abnormality detected at CT and/or MR imaging. If no adenoma was found, a total hypophysectomy was performed (one patient).

All patients were initially evaluated without gadolinium injection. A coronal T1-weighted SE 600/15 (repetition time [TR] msec/echo time [TE] msec) sequence with four excitations was performed in all 28 patients who underwent surgery, and a coronal three-dimensional fast low-angle shot (3D FLASH) (40–70/6, one or two excitations, 32 or 64 partitions) was performed in 27 patients (one technical incident [motion of the patient] occurred). A sagittal T1-weighted SE 600/15 sequence with two averages was performed in 18 patients, and a coronal long-TR SE 2,200–2,500/22 and 90/2 sequence was performed in six patients.

To compare the effect of gadolinium injection in most patients, the postgadolinium T1-weighted sequences (coronal and sagittal T1-weighted SE and 3D FLASH)

Abbreviations: ACTH = adrenocorticotropic hormone, PPV = positive predictive value, SE = spin echo, TE = echo time, 3D FLASH = three-dimensional fast low-angle shot, TR = repetition time.
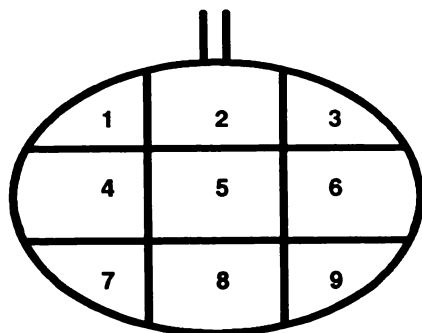
Figure 1. The location of the focal abnormality was defined by dividing the coronal plane of the antehypophysis into nine segments. The coronal diameter of the focal abnormality was measured in millimeters.
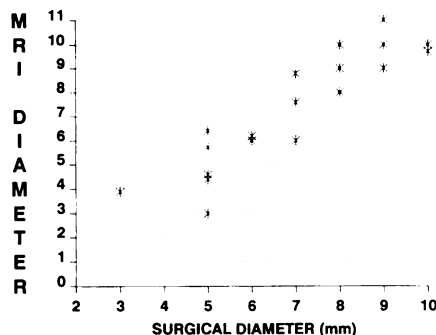

Figure 2. Plot of the diameters of microadenomas on coronal T1-weighted SE images obtained before administration of gadolinium versus the diameters of these microadenomas at surgery. See text for explanation of sensitivity*.

Figure 3. Plot of the diameters of microadenomas on coronal 3D FLASH images obtained before administration of gadolinium versus the diameters of these microadenomas at surgery. See text for explanation of sensitivity*.

Figure 4. Plot of the diameters of microadenomas on coronal T1-weighted SE images obtained after administration of gadolinium versus the diameters of these microadenomas at surgery. See text for explanation of sensitivity*.
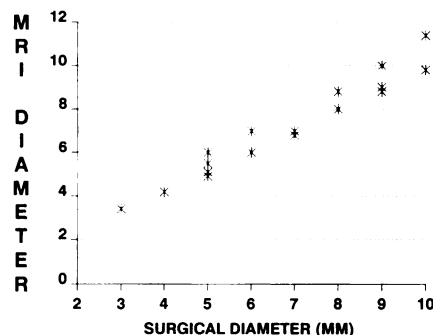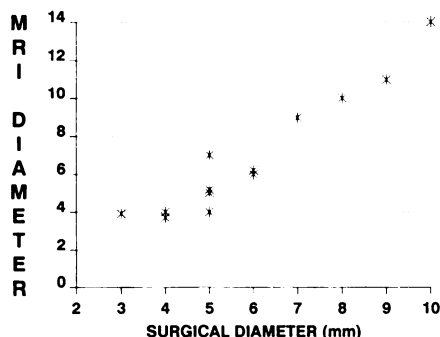

Figure 5. Plot of the diameters of microadenomas on coronal 3D FLASH images obtained after administration of gadolinium versus the diameters of these microadenomas at surgery. See text for explanation of sensitivity*.
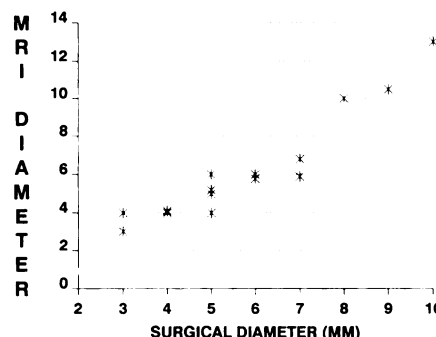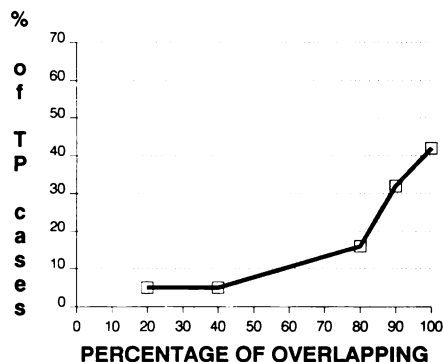

Figure 6. Distribution of the percentage of overlapping of true-positive (*TP*) findings in the coronal cross-sectional area at surgery and findings on coronal T1-weighted SE images obtained before administration of gadolinium in 19 patients.

Figure 7. Distribution of the percentage of overlapping of true-positive (*TP*) findings in the coronal cross-sectional area at surgery and findings on coronal 3D FLASH images obtained before administration of gadolinium in 18 patients.

Figure 8. Distribution of the percentage of overlapping of true-positive (*TP*) findings in the coronal cross-sectional area at surgery and findings on coronal T1-weighted SE images obtained after administration of gadolinium in 13 patients.
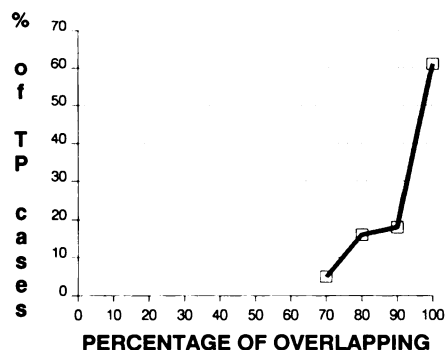

Figure 9. Distribution of the percentage of overlapping of true-positive (*TP*) findings in the coronal cross-sectional area at surgery and findings on coronal 3D FLASH images obtained after administration of gadolinium in 15 patients.
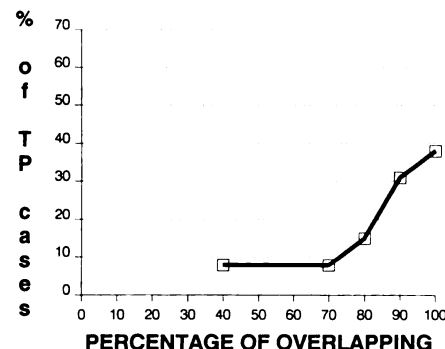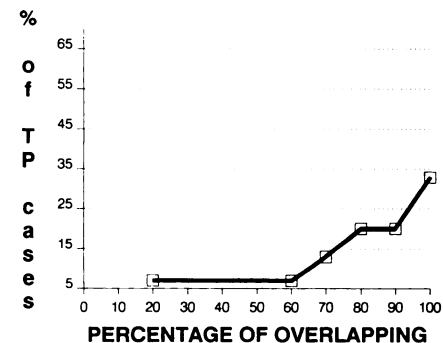
were performed after a period not exceeding 1 week. (In all patients an injection of 113.07 mg/kg tetraazacyclododecanetetraacetic acid [Guerbet, Paris] was performed in 30–60 seconds, and the first sequence [coronal T1-weighted SE] was started immediately after it.) The postgadolinium coronal T1-weighted SE sequence was performed in 24 patients and

was followed by a sagittal T1-weighted SE sequence in 13 patients and/or by a 3D FLASH sequence in 22 patients. The postgadolinium study was not performed in patients whose clinical, CT, and/or MR precontrast imaging data sufficed to enable confident diagnosis.

For all SE sequences the section thick-

ness was 3 mm; for 3D FLASH it was 1.5 mm. For SE sequences 13–15 sections were used; for 3D FLASH, 64 sections were used. All MR examinations were performed with a 1.5-T (Magnetom, Siemens) system with a field of view of 22 cm and a circularly polarized head coil.

Table 1
Results in 28 Patients Who Underwent Surgery

Group	Coronal T1-weighted SE − Gd	Coronal T1-weighted SE + Gd	Coronal 3D FLASH −Gd	Coronal 3D FLASH +Gd	Sagittal T1-weighted SE − Gd	Sagittal T1-weighted SE + Gd	Coronal Proton Density SE	Coronal T2-weighted SE
All 28 patients (27 microadenomas and one multinodular hyperplasia)								
Nex/Nmi	28/27	25/24	27/26	23/22	18/18	13/13	6/6	6/6
No. of true-positive imaging examinations	19	13	18	15	11	7	3	2
Sensitivity (%)	70	54	69	68	61	54	50	33
Positive predictive value (%)	90	87	78	83	73	64	100	100
No. of false-positive imaging examinations	2	2	5	3	4	4	0	0
Prolactinomas (20 patients, 20 microadenomas)								
Nex/Nmi	20/20	19/19	20/20	17/17	14/14	11/11	4/4	4/4
No. of true-positive imaging examinations	14	9	14	11	9	5	1	1
Sensitivity (%)	70	47	70	64	64	45	ND	ND
Positive predictive value (%)	88	82	82	92	90	63	ND	ND
No. of false-positive imaging examinations	2	2	3	1	1	3	0	0
Cushing disease (seven patients; six microadenomas and one multinodular hyperplasia)								
Nex/Nmi	7/6	6/5	6/5	6/5	4/4	2/2	1/1	1/1
No. of true-positive imaging examinations	4	4	4	4	3	2	0	1
Sensitivity (%)	67	80	80	80	ND	ND	ND	ND
Positive predictive value (%)	100	100	67	67	ND	ND	ND	ND
No. of false-positive imaging examinations	0	0	2	2	1	0	0	0
Growth hormone secretion (one patient, one microadenoma)								
Nex/Nmi	1/1	ND	1/1	ND	ND	ND	1/1	1/1
No. of true-positive imaging examinations	1	ND	0	ND	ND	ND	1	1
No. of false-positive imaging examinations	0	ND	0	ND	ND	ND	0	0

Note.—The microadenoma was found in 27 patients. In one patient with Cushing disease, only multinodular hyperplasia was found. The sensitivity calculations apply only to a specific group of surgical patients with positive results of examination with CT and/or MR imaging. —Gd = before administration of gadolinium, +Gd = after administration of gadolinium, ND = no data, Nex/Nmi = no. of patients examined with a given sequence/no. of microadenomas found at surgery.

The 3D FLASH studies were performed with a 40° flip angle and a 96-mm-thick three-dimensional volume.

The location and size of the focal abnormality were prospectively evaluated by two neuroradiologists in agreement about its presence (Fig 1). Secondary signs of mass effect were not taken into account for this evaluation. All transsphenoidal explorations were performed by a single neurosurgeon, who evaluated the location and size of microadenomas by using the scheme in Figure 1. With these data, the capability of different sequences to enable location and measurement of the diameter of microadenomas was evaluated with three considerations in mind:

1. Positive predictive value (PPV) = (number of patients with an adenoma and positive test results)/(number of patients with positive test results), and sensitivity = (number of patients with an adenoma and positive test results)/(number of patients with adenoma). (Because the findings at MR imaging influenced the selection of patients for surgery, the PPV was calculated. The sensitivity calculations apply only for a specific group of postsurgical patients with positive CT and/or MR findings. In other words, patients who had microadenomas without typical hormonal secretion and without focal lesions on CT scans and/or MR images did not undergo surgery, so that results for the sensitivity* values were biased [marked with * for these reasons]. If the number of imaging examinations used to calculate PPV and sensitivity* was equal to or lower than four, only the number of true-positive results and the number of false-positive results were recorded. For the same reasons, the negative predictive value and the specificity* were not calculated either [only one patient had no adenoma at surgery]).

2. A scatter plot was made of the diameters of microadenomas at surgery versus the diameters of these microadenomas at examination with coronal T1-weighted SE images obtained before the administration of gadolinium (Fig 2), coronal 3D FLASH images obtained before the administration of gadolinium (Fig 3), coronal T1-weighted SE images obtained after the administration of gadolinium (Fig 4), and coronal 3D FLASH images obtained after the administration of gadolinium

(Fig 5).

3. The distribution of the true-positive MR imaging findings was determined on the basis of the percentage of overlapping between the surgical and MR imaging findings (Figs 6–9).

The finding of a focal abnormality was considered true positive only when at least 20% of the lesion on the surgeon's anatomic grid overlapped the lesion on the MR image and the side (left or right) of the location was the same on both the grid and the MR image. Otherwise, the finding was considered false positive in conjunction with false negative. The presence of a second focal abnormality distant from the true-positive one was considered false positive in conjunction with a true-positive finding.

Furthermore, we investigated combinations of sequences to find out which provided the highest rate of true-positive findings and the lowest rate of false-positive findings.

RESULTS

The results are summarized in Table 1.

Patients with Adenoma at Surgery

The best sensitivity* was achieved, in decreasing order, with these sequences: pregadolinium coronal T1-weighted SE (70%), pregadolinium coronal 3D FLASH (69%), postgadolinium coronal 3D FLASH (68%), pregadolinium sagittal T1-weighted SE (61%), postgadolinium coronal and sagittal T1-weighted SE (54%), coronal long-TR short-TE SE (50%), and coronal long-TR long-TE SE (33%). The low signal intensity of the long-TR SE sequence explains the absence of false-positive examinations, low sensitivity,* and high PPV. Furthermore, this sequence was performed only in six patients. For other sequences, the highest PPV was achieved with coronal pregadolinium T1-weighted SE (90%) and coronal postgadolinium T1-weighted SE (87%) images. The capability to evaluate the diameter of the microadenoma with the most effective techniques (pre- or postgadolinium coronal T1-weighted SE and coronal 3D FLASH sequences) is represented on a scatter plot of diameters measured at MR imaging versus diameters measured at surgery (only true-positive cases) (Figs 2–5). The general accuracy of diameter measurement for true-positive cases was very good when pre- or postgadolinium coronal T1-weighted SE and 3D FLASH images were used.

The maximum error never exceeded 2 mm, except for a prolactinoma with a diameter of 10 mm, recorded as 14 mm when a coronal postgadolinium T1-weighted SE sequence was used and as 13 mm when a coronal postgadolinium 3D FLASH sequence was used. The lowest dispersion of MR imaging measurements was observed with use of pregadolinium coronal 3D FLASH images (Fig 3). The capability to evaluate the location of the microadenoma with the most effective sequences (pre- or postgadolinium coronal T1-weighted SE and 3D FLASH sequences) is represented on a plot of the distribution of the percentage of patients with true-positive findings versus the percentage of overlap between findings at MR imaging and findings at surgery (Figs 6–9). The best results are achieved with coronal pregadolinium 3D FLASH images (61% of true-positive cases had 100% overlapping between the findings at MR imaging and the findings at surgery [Fig 7]) and coronal pregadolinium T1-weighted SE images (41% of true-positive cases had 100% overlapping between findings at MR imaging and

Table 2
Effect of Sequence Combination on Findings

Combination of Coronal Sequences	No. of True-Positive Findings	No. of False-Positive Findings
T1 SE − Gd	14 (66.6)	1 (4.7)
T1 SE + Gd	11 (52.3)	2 (9.5)
3D FLASH − Gd	15 (71.4)	3 (14.3)
3D FLASH + Gd	15 (71.4)	2 (9.5)
T1 SE − Gd 3D FLASH − Gd	16 (76.2)	1 (4.7)
T1 SE − Gd T1 SE + Gd	17 (81)	1 (4.7)
T1 SE − Gd 3D FLASH − Gd T1 SE + Gd	18 (85.7)	1 (4.7)
T1 SE − Gd 3D FLASH − Gd T1 SE + Gd 3D FLASH + Gd	19 (90.4)	1 (4.7)

Note.—The statistics were calculated in 21 patients for whom all four sequences were performed. Numbers in parentheses are percentages. T1 SE − Gd = coronal T1-weighted SE sequence performed before administration of gadolinium, T1 SE + Gd = coronal T1-weighted SE image obtained after administration of gadolinium, 3D FLASH − Gd = coronal 3D FLASH image obtained before administration of gadolinium, 3D FLASH + Gd = coronal 3D FLASH image obtained after administration of gadolinium. Positive predictive value for the combination of all four sequences was 95%.

Table 3
Positive and Negative Yield of Gadolinium Injection in Patients Who Underwent Coronal T1-weighted SE and 3D FLASH Imaging Studies

Sequence	No. of True-Positive Findings in Pregadolinium Sequence	Positive Yield in False-Negative Cases	Negative Yield in True-Positive Cases
Coronal T1-weighted SE (24 patients)	16 (67)	3 (38)	6 (38)
Coronal 3D FLASH (21 patients)	15 (71)	2 (33)	5 (33)

Note.—The statistics were calculated in the patients who underwent pre- and postgadolinium studies. Numbers in parentheses are percentages.

the findings at surgery [Fig 6]). The relationship between the surgical diameter of the microadenoma and the sensitivity* of the study was also evaluated for the pregadolinium coronal T1-weighted SE images and 3D FLASH images. The sensitivity * improved with the increasing size of the microadenoma (100% sensitivity in microadenomas with diameters of 9 mm or greater imaged with both sequences), but the sensitivity* to small adenomas (3 mm in diameter) was higher in 3D FLASH images (50%) than in T1-weighted SE images (30%). When we considered combinations of different sequences performed in 21 patients for whom all four sequences were performed (Table 2), the best results in the detection of microadenomas were achieved with the combination of pre- and postgadolinium coronal T1-

weighted SE images with pre- and postgadolinium coronal 3D FLASH images (PPV = 95%, number of true-positive findings = 19 [90%], number of false-positive findings = 1 [5%]). The combination of pre- and postgadolinium coronal T1-weighted SE images with pregadolinium coronal 3D FLASH images produced true-positive results in 85.7% of MR imaging examinations; the combination of pre- and postgadolinium coronal T1-weighted SE images produced true-positive results in 81% of MR imaging examinations (Table 2). There was no improvement in the detection of microadenomas by addition of sagittal pre- and postgadolinium T1-weighted SE images and long-TR SE images to the most efficient combination of the sequences (pre- and postgadolinium coronal T1-weighted SE and 3D FLASH).
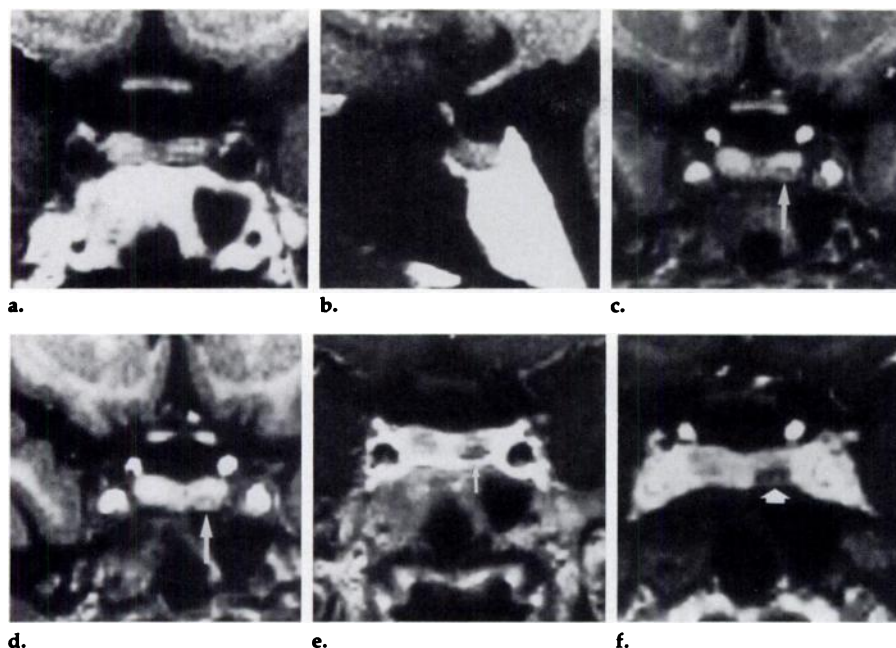
Figure 10. ACTH-secreting microadenoma 4 mm in diameter. (a) False-negative coronal T1-weighted SE, (b) false-negative sagittal T1-weighted SE, and (c, d) coronal 3D FLASH images without administration of gadolinium. (e) Coronal T1-weighted SE and (f) coronal 3D FLASH images obtained after administration of gadolinium. On pregadolinium studies (a–d), a low-contrast area of focal hypointensity (arrow, c and d) can only be suspected, especially with a 3D FLASH sequence (c, d) (the pregadolinium studies were insufficient to enable a confident diagnosis). After injection of gadolinium, the microadenoma (arrow, e and f) is as clearly visualized on the T1-weighted SE image (e) as on the 3D FLASH image (f). Nevertheless, the contrast between the hypophysis and microadenoma is greater on the 3D FLASH image (6.6 for the SE image and 8.6 for the 3D FLASH image). (The contrast was calculated with the following equation: Contrast = [signal intensity of hypophysis − signal intensity of microadenoma]/noise.)

Patient without Adenoma at Surgery

In one patient with cyclic Cushing disease, only nodular hyperplasia without evidence of microadenomas was found. The coronal pre- and postgadolinium SE images as well as CT scans were normal in this patient. The pre- and postgadolinium 3D FLASH images showed a focal hypointensity but did not enable confident diagnosis. So, in this patient, the SE images and CT scans resulted in a true-negative evaluation and the 3D FLASH sequence in a false-positive one. Nevertheless, after a subtotal hypophysectomy, the patient's levels of ACTH have been normal for longer than 1 year; whether this is of hypothalamic or pituitary origin is still dubious.

Effects of Gadolinium Injection

Statistical analysis of the effects of contrast material injection was performed in the patients who underwent pre- and postgadolinium studies (SE images were obtained in 24 patients and 3D FLASH images were obtained in 21 patients). After injection of gadolinium, the microadenoma could be detected in three of eight patients who had false-negative T1-weighted SE images (resulting in a positive yield of 37.5%) (positive yield of gadolinium in the microadenomas negative on the pregadolinium images = [number of positive cases on postgadolinium images but negative on pregadolinium images]/[number of cases negative on pregadolinium images]) and in two of

six patients with false-negative 3D FLASH images (positive yield of 33.3%) (Table 3). Of 16 true-positive findings on pregadolinium coronal T1-weighted SE images, six became false negative after injection of gadolinium (negative yield of 37.5%) (negative yield of gadolinium in the microadenomas positive on the pregadolinium scans = [number of negative cases on postgadolinium scans but positive on pregadolinium scans]/[number of positive cases on pregadolinium scans]), and of 15 true-positive findings on pregadolinum coronal 3D FLASH images, five became false negative after injection of gadolinium (Table 3).

DISCUSSION

Recent studies of MR imaging in the diagnosis of pituitary microadenomas still vary in their evaluation of diagnostic accuracy and the most useful sequence parameters of this modality. Our study, performed at 1.5 T, demonstrates the utility of three-dimensional acquisition (Figs 10–12) and coronal T1-weighted SE images without gadolinium in the diagnosis of microadenomas. The highest sensitivity was achieved with coronal pregadolinium T1-weighted SE images (70%) and coronal pregadolinium 3D FLASH images (69%). Recent studies done with a 1.5-T magnet and 3-mm thick sections (Table 4) also suggest a high accuracy of T1-weighted sequences. Kucharczyk et al (3) imaged 10 of 11 ACTH-secreting microadenomas (91%), Kulkarni et al (4) imaged eight of eight microadenomas (100%), Peck et al (1) im-

aged 17 of 21 ACTH-secreting microadenomas (81%), and Nichols et al (2) imaged nine of 11 (six ACTH- and five prolactin-secreting) microadenomas (82%). Nevertheless, there are also reports of a lower accuracy of unenhanced 1.5-T images. Pojunas et al (9) failed to detect five of 11 prolactinomas (45%), and Doppman et al (6) failed to detect five of eight ACTH-secreting microadenomas (62%). The poor results of some studies can, at least in part, be explained by technical parameters (ie, an insufficient number of excitations [one or two] and a small [128-pixel] matrix) (Table 4).

The good results of 3D FLASH images can be explained by the use of smaller sections in 3D FLASH images and by good optimization of this sequence for pituitary examinations. (After the influence of TR, flip angle, and number of partitions versus total acquisition volume and number of excitations have been evaluated, the best results in imaging the hypophysis with 3D FLASH are achieved with the following parameters: 70/6, one excitation, 64 sections of 1.5 mm thickness, and zoom of 1.2. The technical factors of MR imaging equipment are also important in achieving a good contrast-to-noise ratio in three-dimensional imaging of the hypophysis (including a circularly polarized head coil with a high signal-to-noise ratio, strong gradients allowing the use of short TE, and high homogeneity of the magnetic field).

Nevertheless, in suboptimal conditions (motion artifacts induced by poor cooperation from the patient, for example, or a highly pneuma-
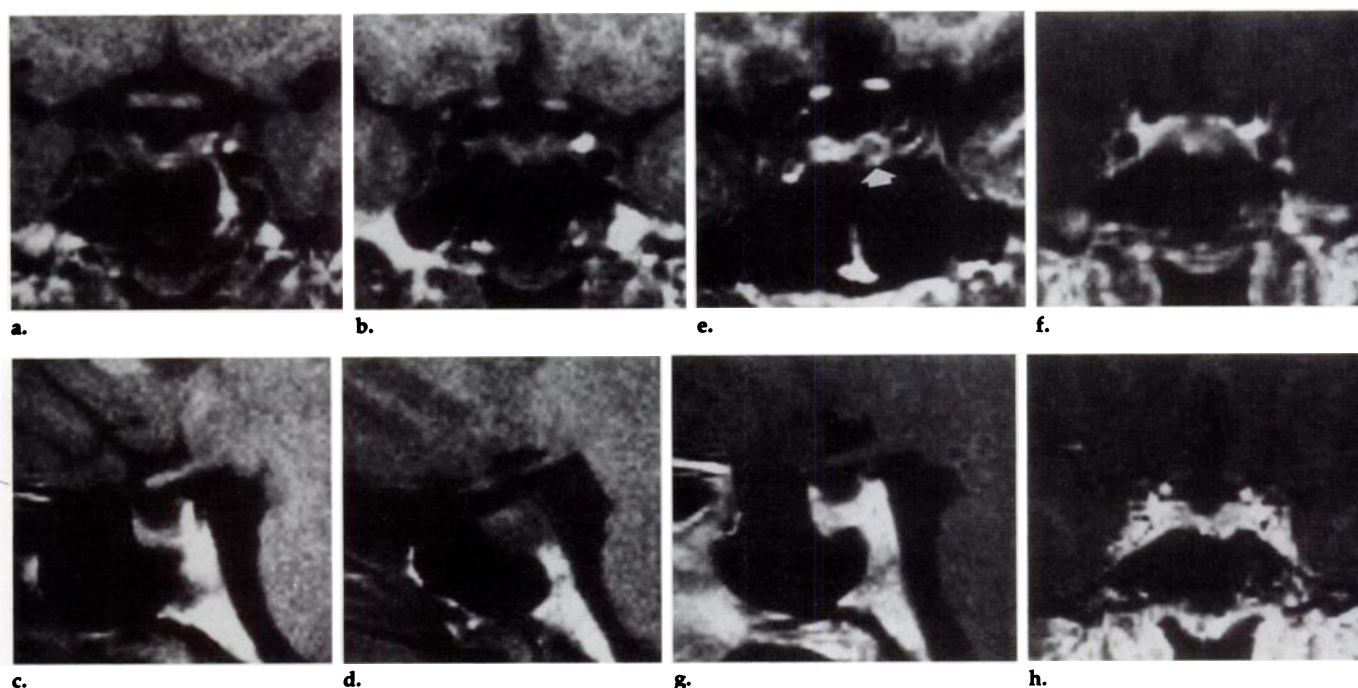
Figure 11. Prolactinoma 3–4 mm in diameter that was treated with bromocriptine. (a, b) Two contiguous sections of coronal T1-weighted SE sequence and (c, d) two contiguous sections of sagittal T1-weighted SE sequence, at the level of the microadenoma. (e) Coronal 3D FLASH image obtained without administration of gadolinium. (f) Coronal T1-weighted SE, (g) sagittal T1-weighted SE, and (h) coronal 3D FLASH images obtained after administration of gadolinium (f–h were obtained at the level of the microadenoma). This small microadenoma (arrow, e), treated with bromocriptine, could be visualized only with 3D FLASH without administration of gadolinium. All other pre- or postcontrast sequences, as well as CT, were unable to demonstrate it.

Table 4
Parameters for T1-weighted MR Imaging of Microadenomas at 1.5 T

Study	Sequence	TR (msec)	TE (msec)	No. of Signals Averaged	Matrix	Gap (mm)	Section Thickness (mm)	True-Positive Rate (%)	No. of Patients who Underwent Surgery
Kucharczyk et al (3)	SE	600	25	6	256	0	3	91	11
Kulkarni et al (4)	SE*	2000–3000	20, 30–70, 80	2	128	0.6	3	100	8
	IR†	2500	20	2	128	0.6	3		
Peck et al (1)	SE	600	20	4	256	0.3	3	81	21
Pojunas et al (9)	SE	300–800	14–25	1 or 2	128 or 256	0	3	54	11
Doppman et al (6)	SE	600	20	2	256	0	3	38	8
Nichols et al (2)	SE	500	20	4	256	0.6	3	81	11

Note.—IR = inversion recovery.
* Performed with electrocardiographic gating.
† Inversion time = 800 msec.

tized sphenoid sinus that induces susceptibility artifacts), the homogeneity of the three-dimensional study can be significantly lower than that of a conventional SE study, hence the higher number of false-positive examinations and the lower number of confident diagnoses with respect to conventional SE studies.

The few reports about the diagnostic utility of gadolinium studies at 1.5 T suggest a higher accuracy of postcontrast studies (5–8). In a series of eight ACTH-secreting microadenomas imaged at 1.5 T, Doppman et al (6) achieved accuracy rates of 38% for true-positive precontrast studies and 50% for true-positive postcontrast studies. Nevertheless, only two averages and a rather long TE of 20 msec were used in this study. Davis et al (5) found postgadolinium studies superior in two of three microadenomas but used only a 0.5 T MR imaging unit and a 5-mm section thickness. The study of Dwyer et al (7) (in which 13 ACTH-secreting microadenomas were imaged) reported that eight of 12 surgically confirmed microadenomas were seen on pregadolinium studies and none were seen on postgadolinium studies. Dwyer et al also used a 0.5-T MR imaging unit and a 5-mm section thickness. In our experience, when evaluated separately, the pregadolinium studies enabled greater diagnostic accuracy than the postgadolinium studies. This can be explained by technical factors discussed in Patients and Methods. These factors allow the visualization of microadenomas which, when lower-resolution equipment is used, can be visualized only after administration of gadolinium (Fig 13). Another factor can be a flip-flop from dark to bright after injection of gadolinium, with a frequent period of isointensity between the hypophysis and microadenoma during which the presence of gadolinium may obscure rather than help to visualize the lesion (7) (Figs 14, 15). In our experience the negative yield after injec-
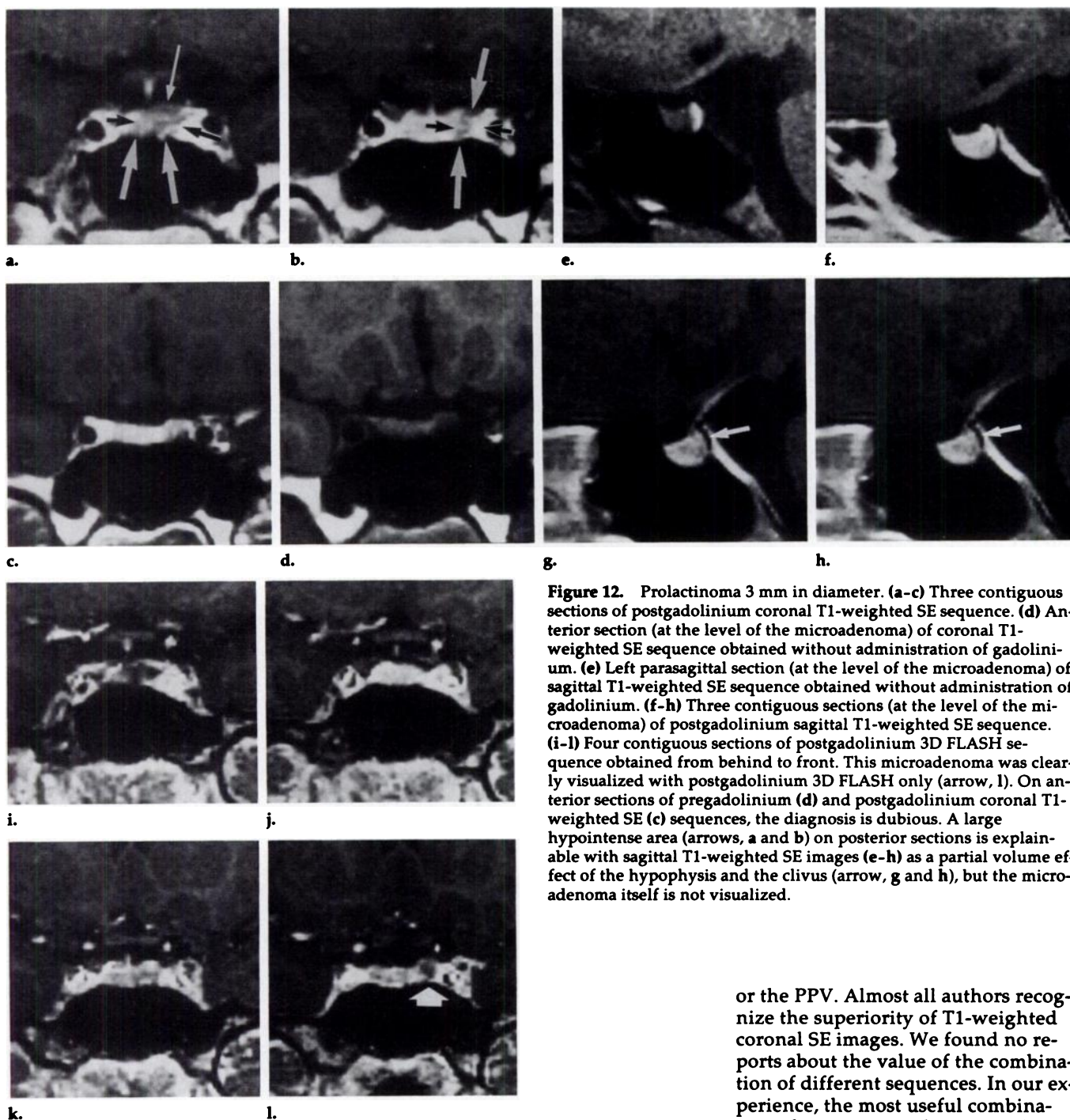
Figure 12. Prolactinoma 3 mm in diameter. (a-c) Three contiguous sections of postgadolinium coronal T1-weighted SE sequence. (d) Anterior section (at the level of the microadenoma) of coronal T1-weighted SE sequence obtained without administration of gadolinium. (e) Left parasagittal section (at the level of the microadenoma) of sagittal T1-weighted SE sequence obtained without administration of gadolinium. (f-h) Three contiguous sections (at the level of the microadenoma) of postgadolinium sagittal T1-weighted SE sequence. (i-l) Four contiguous sections of postgadolinium 3D FLASH sequence obtained from behind to front. This microadenoma was clearly visualized with postgadolinium 3D FLASH only (arrow, l). On anterior sections of pregadolinium (d) and postgadolinium coronal T1-weighted SE (c) sequences, the diagnosis is dubious. A large hypointense area (arrows, a and b) on posterior sections is explainable with sagittal T1-weighted SE images (e-h) as a partial volume effect of the hypophysis and the clivus (arrow, g and h), but the microadenoma itself is not visualized.

tion of gadolinium was 37.5% for coronal T1-weighted SE images and 33.3% for coronal 3D FLASH images. The positive yield after injection of gadolinium was 37.5% for coronal T1-weighted SE images and 33.3% for coronal 3D FLASH images.

Our results agree with the previously reported limited value of sagittal T1-weighted SE images (especially because of the high rate of false-positive findings) and long-TR SE images (1,4,6,9). In our study, the sensitivity* of long-TR SE images was low (Fig 13), and the combination with other sequences never improved the
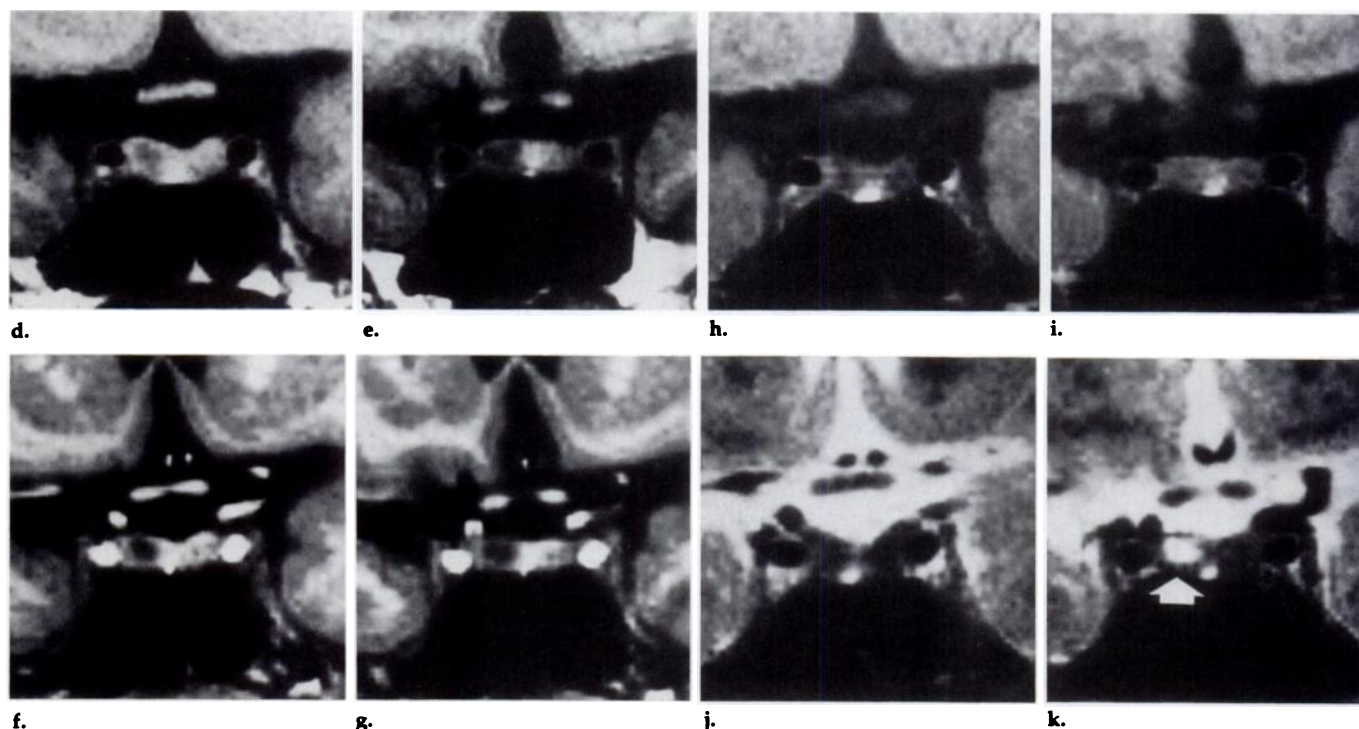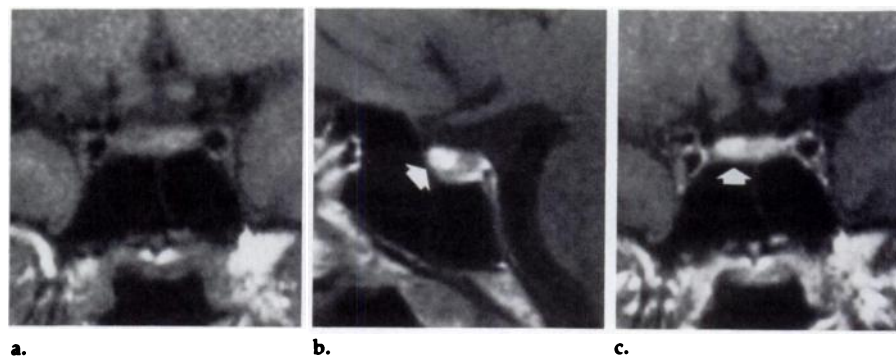
total sensitivity. Nevertheless, these sequences were performed only in six patients who underwent surgery.

We agree with Peck et al (1) that the sagittal T1-weighted SE image is also of limited value because of partial volume artifacts caused by the carotid artery and difficulties in comparing the left and right parts of the hypophysis.

The combination of sagittal pre- and postgadolinium studies with coronal pre- and postgadolinium T1-weighted SE studies and coronal pre- and postgadolinium 3D FLASH studies has not improved the sensitivity

or the PPV. Almost all authors recognize the superiority of T1-weighted coronal SE images. We found no reports about the value of the combination of different sequences. In our experience, the most useful combination of sequences is the pre- and postgadolinium coronal T1-weighted SE image with the pre- and postgadolinium 3D FLASH image. This combination produced the highest number of true-positive cases (90.4%) and the lowest number of false-positive cases (4.7%). The two false-negative cases (incidentally also false negative at CT) were the prolactinomas treated with Parlodel (bromocriptine mesylate; Sandoz, Parsippany, NJ) (Fig 16).

Therefore, the precontrast sequences that were evaluated separately gave a higher accuracy than the postcontrast ones, but the combination of both allows the highest accuracy. The CT scans in our study
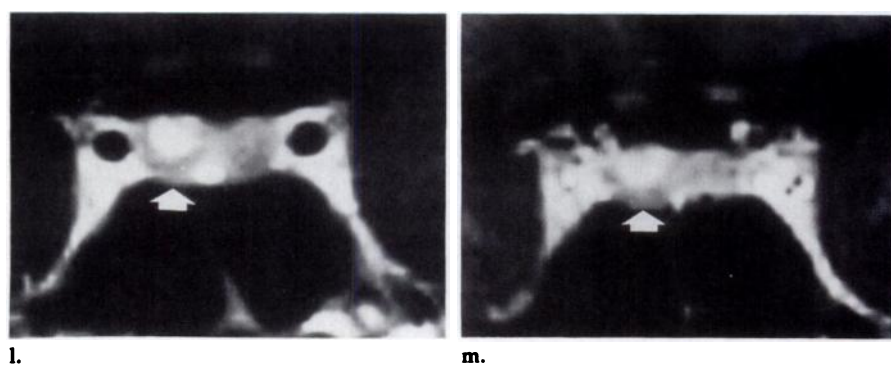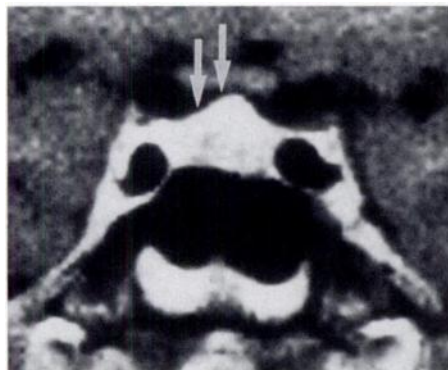
Figure 13. ACTH-secreting microadenoma 4 mm in diameter. (a) Coronal pregadolinium T1-weighted SE image. (b) Sagittal postgadolinium T1-weighted SE image. (c) Coronal post-gadolinium T1-weighted SE image. These images (a-c) were obtained with a 1.5-T magnet, a 3-mm section thickness, four averages, TR of 450 msec, and TE of 30 msec. The hyperintense focal lesion (arrow, b and c) is poorly demonstrated on postgadolinium sequences only. (d, e) Coronal pregadolinium T1-weighted SE images obtained at levels 5.4 (d) and 8.4 (e). (f, g) Coronal pregadolinium 3D FLASH images obtained at levels 6.9 (f) and 8.4 (g). (h, i) Coronal proton-density SE images obtained by means of a 2.3/22 sequence with two averages at levels 5.4 (h) and 8.4 (i). (j, k) Coronal T2-weighted SE images obtained by means of a 2,300/90 sequence with two averages at levels 5.4 (j) and 8.4 (k). (l) Coronal postgadolinium T1-weighted SE image. (m) Coronal postgadolinium 3D FLASH image. These images (d-m), obtained at our institution 2 months after a-c were obtained, clearly demonstrate a microadenoma on pregadolinium T1-weighted SE images (d, e) and 3D FLASH images (f, g) as an area of focal hypointensity. (Note higher contrast between hypophysis and ade-noma on 3D FLASH images.) On the postgadolinium T1-weighted SE image (l) and 3D FLASH image (m) the microadenoma was hyperintense (arrow, l and m). The long-TR se-quences (h-k) have a limited value. Indeed, only the anterior, probably more cystic, part of the microadenoma (arrow) can be visualized on the T2-weighted SE image (k).
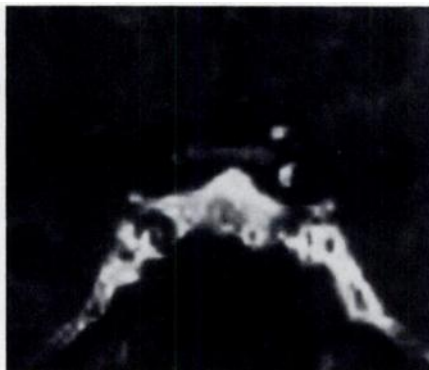
were heterogeneous, most of them having been obtained in other hospi-tals; they were not included in our evaluation.

CONCLUSION

For a 1.5-T MR imaging unit with a high signal-to-noise ratio that allows useful three-dimensional acquisi-tions, we advocate the following scheme of sequences for the diagno-sis of pituitary microadenomas: a cor-onal T1-weighted SE sequence fol-lowed by a coronal 3D FLASH se-quence (if the coronal T1-weighted SE sequence does not allow the diag-nosis), both without injection of gad-olinium. When confident diagnosis still is not reached, the same se-quences should be performed after the injection of gadolinium. The sag-ittal T1-weighted SE sequence (with or without injection of gadolinium) and long-TR SE sequence are useful only in specific cases. The high-field-strength MR imaging unit with a

a.

b.

high signal-to-noise ratio and three-dimensional capabilities enables sensitive imaging for presurgical evaluation of pituitary microadenomas. ∎

References

1. Peck WW, Dillon WP, Norman D, Newton TH, Wilson CB. High-resolution MR imaging of pituitary microadenomas at 1.5T: experience with Cushing disease. AJR 1989; 152:145–151.

c.

d.

Figure 14. Prolactinoma 9 mm in diameter. (a) Coronal T1-weighted SE and (b) coronal 3D FLASH images obtained without administration of gadolinium. (c) Coronal T1-weighted SE and (d) coronal 3D FLASH images obtained after administration of gadolinium. This adenoma was correctly evaluated only with precontrast studies (a, b); it is more conspicuous on b. On the postcontrast SE image (c), only the displacement of the diaphragm (arrows) is visualized. (No focal abnormality is seen; this image was considered false negative.) In d, only a central hypointensity (probably a more necrotic area) can be distinguished (this image was considered true positive).
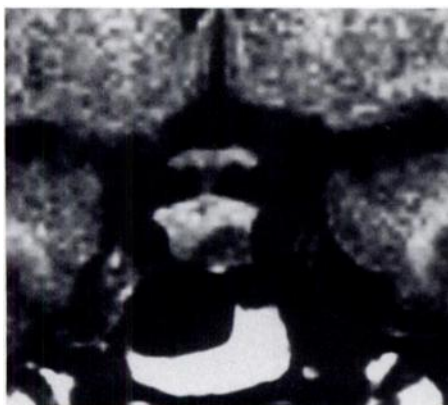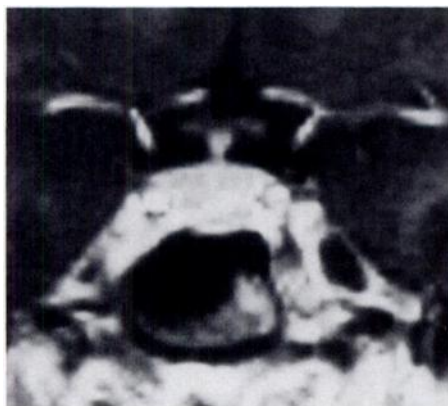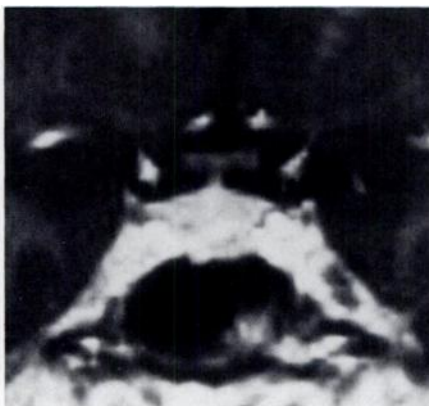
a.
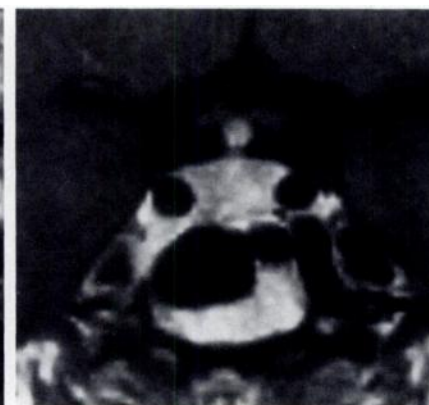
b.

c.

d.

e.

Figure 15. Prolactinoma 8–9 mm in diameter. (a) Coronal T1-weighted SE image obtained without administration of gadolinium. (b) Coronal T1-weighted SE image obtained after administration of gadolinium. (c) Sagittal T1-weighted SE image obtained after administration of gadolinium. (d, e) Coronal 3D FLASH images (two contiguous sections) obtained after administration of gadolinium. This prolactinoma was clearly visualized with all precontrast sequences (coronal T1-weighted SE [a], sagittal T1-weighted SE, and coronal 3D FLASH). Because of a sudden reversal in contrast (from dark to light) after administration of gadolinium, the prolactinoma could not be visualized with postcontrast sequences (b–e).
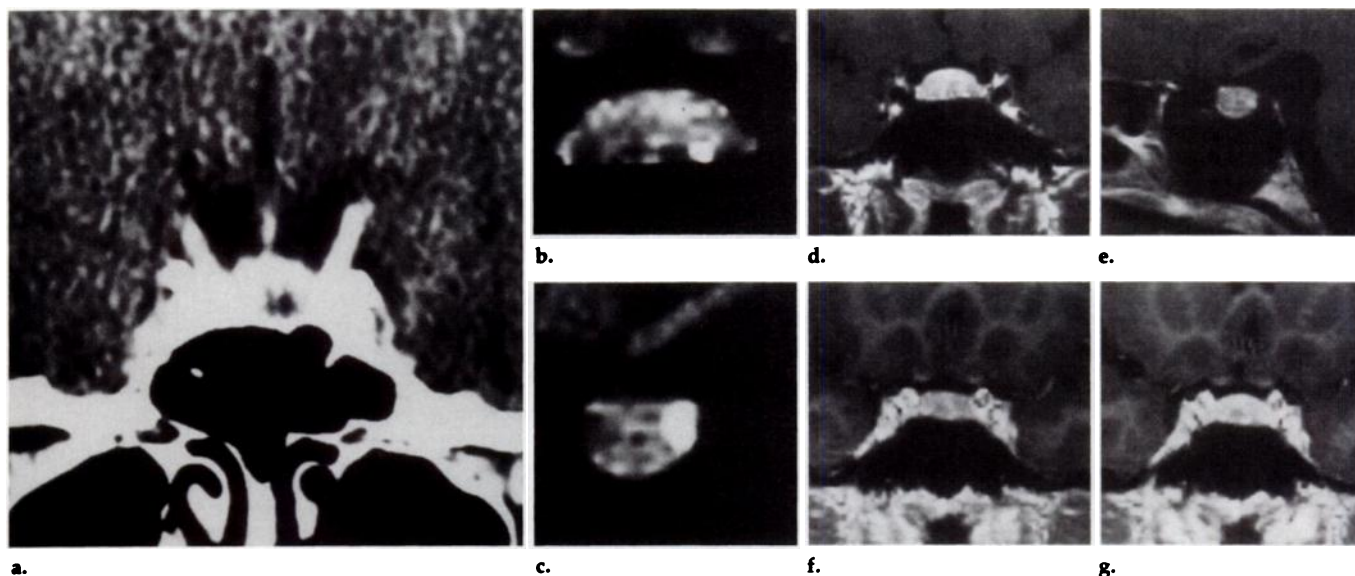
Figure 16. Fibrotic prolactinoma 6 mm in diameter in a patient who received bromocriptine treatment for 3 years. **(a)** CT scan obtained before treatment. **(b)** Coronal pregadolinium T1-weighted SE image. **(c)** Sagittal pregadolinium T1-weighted SE image. **(d)** Coronal postgadolinium T1-weighted SE image. **(e)** Sagittal postgadolinium T1-weighted SE image. **(f, g)** Two contiguous sections of postgadolinium 3D FLASH study. All these sections **(b-g)** were made at the level of the microadenoma, which was seen only on the first, pretreatment CT scan **(a)**. The consecutive CT scans and MR images **(b-g)** were false negative.

2. Nichols DA, Laws ER, Houser OW, Abboud CF. Comparison of magnetic resonance imaging and computed tomography in the preoperative evaluation of pituitary adenomas. Neurosurgery 1988; 22:380–385.
3. Kucharczyk W, Davis DO, Kelly WM, Sze G, Norman D, Newton TH. Pituitary adenomas: high-resolution MR imaging at 1.5 T. Radiology 1986; 161:761–765.
4. Kulkarni MV, Lee KF, McArdle CB, Yeakley JW, Haar FL. 1.5-T imaging of pituitary microadenomas: technical consider-

ations and CT correlations. AJNR 1988; 9:5–11.
5. Davis PC, Hoffman JC, Malko JA, et al. Gadolinium-DTPA and MR imaging of pituitary adenoma: a preliminary report. AJNR 1987; 8:817–823.
6. Doppman JL, Frank JA, Dwyer AJ, et al. Gadolinium DTPA enhanced MR imaging of ACTH-secreting microadenomas of the pituitary gland. J Comput Assist Tomogr 1988; 12:728–735.
7. Dwyer AJ, Frank JA, Doppman JL, et al. Pituitary adenomas in patients with Cush-

ing disease: initial experience with Gd-DTPA–enhanced MR imaging. Radiology 1987; 163:421–426.
8. Steiner VE, Wimberger D, Imhof H, Knosp E, Hajek P. Gd-DTPA in MR diagnosis of pituitary adenomas. ROFO 1989; 150:323–327.
9. Pojunas KW, Daniels DL, Williams AL, Haughton VM. MR imaging of prolactin-secreting microadenomas. AJNR 1986; 7:209–213.